Laser Emission Characteristics of Dye-Doped Cholesteric Films

Th. K. Mavrogordatos, S. M. Morris, P. J. W. Hands and T. D. Wilkinson

Centre of Molecular Materials for Photonics and Electronics (CMMPE), Department of Engineering, University of Cambridge

Abstract: This paper aims to give an overview of distributed feedback (DFB) lasing in chiral nematic liquid crystals (CLC) and explain the salient features that render them unique. Particular emphasis is given to the transmission and reflection characteristics of CLCs as well as to the key role of the Density of Photon States (DOS) in the presence of an active medium. Discussions and comparisons with wave propagation in other periodic solid media are also included.

1. Introduction

Recently, there has been an explosion of interest in band-edge lasing in chiral liquid crystals (LC), which is related to the low-excitation threshold and tuneability of the band-gap when a LC is subjected to a variety of different external stimuli. Distributed Feedback (DFB) lasing occurs at frequencies close to the stop-band edges that are associated with the so called band-edge lasing modes[1,2]. As mentioned in [1], the case of CLCs is unique when compared to other conventional periodic media, as an exact solution of Maxwell's equations exists owing to their unusual optical properties. Thus, a boundary value problem can be formulated for non-absorbing, absorbing and amplifying Chiral LCs with analytic solutions. In this paper we follow and expand the methodologies presented in [1,2,3] attempting to link our results with experimental data given in [4,5] .

2. Wave propagation in CLCs: transformed frames and 'reduced indices'

In the chiral nematic phase the director precesses continuously and orthogonally along a single direction (coinciding with the $z-axis$ in our case) giving rise to a helical structure. A full rotation of the director determines the helix pitch p. In [2] de Vries introduces a rotating frame of reference following the precessions of the director, which is schematically shown in [3] alongside transformation relations to the Cartesian frame. In that rotating frame, the eigenwaves have the z dependence $exp(jk_i z), i = 1,2\ and\ j^2 = -1$ with

$$k_i = 2\pi \frac{m_i'}{\lambda' p}, i = 1,2 \quad \textbf{(2.1)} \quad \text{and} \quad m_i'^2 = \frac{m_i^2}{\bar{n}_0{}^2} = 1 + \lambda'^2 \mp \sqrt{4\lambda'^2 + a^2}\,, i = 1(-), 2(+) \quad \textbf{(2.2)}$$

The preceding relation defines the so called 'reduced refractive indices' that are a consequence of the introduction of the rotating frame when applying Maxwell's equations in the CLC cell. The ordinary and extraordinary refractive indices enter the relations through the reduced wavelength $\lambda' = \lambda/(\bar{n}_0 p)$ **(2.3)** with $\bar{n}_0 = \sqrt{(1/2)\left(n_\perp^2 + n_\parallel^2\right)}$ **(2.4)** and $a = (n_\parallel^2 - n_\perp^2)/(2\bar{n}_0{}^2)$ **(2.5)** .The eigenwaves have elliptical polarisations in general, as shown by their corresponding unit vectors $\hat{e}_i = \frac{1}{\sqrt{1+|f_i|^2}}\left(\hat{\xi} + j f_i \hat{\eta}\right), i = 1,2$ **(2.6)**. The parameter f_i is the ellipticity factor that reflects changes in the polarisation of the normal modes as the wavelength varies. As we can observe, for specific wavelengths, the reduced index m_i' that corresponds to the first eigenwave is imaginary, setting the limits of the stop band exhibited by the periodic structure (of infinite length). At the edges of the stop band, the ellipticity factor is either zero or tends to infinity giving rise to a linearly polarised wave (in the rotating frame) that is perpendicular or parallel to the director respectively $\left(\hat{n} \equiv \hat{\eta} \perp \hat{\xi}\right)$. In the laboratory frame this corresponds to a circularly polarised wave. As the (finite) number of the director precessions (N) decreases, the distance between the two minima of the reflection coefficient either side of the band-gap broadens: this is a result that is also derived in [1] whereby the distance between successive edge modes is inversely proportional to the square of the cell thickness.

3. Density of (photon) states (DOS): definition and importance

By invoking *Fermi's Golden Rule*, in the semi-classical approach, the photon emission rate of light with a certain polarisation and wave vector $\vec{k}$ from an excited fluorescent molecule is $w_i \sim \rho_i \left|\langle \psi_{final} | \vec{\mu} \cdot \vec{A}_k | \psi_{initial} \rangle\right|^2,\ i = 1,2$ **(3.1)** where ρ_i is the density of states for the normal mode i, $\vec{\mu}$ is the electric dipole moment, $\vec{A}_k$ is the electromagnetic vector potential corresponding to the plane monochromatic electromagnetic wave with wave vector $\vec{k}$,that represents the perturbation (related to the eigenfield of the normal modes supported by the structure, $\vec{E}_1$ and $\vec{E}_2$) and $\psi_{final}, \psi_{initial}$ denote the wave functions of the initial and final state between which the transition occurs. The above expression can be written as $w_i \sim \rho_i \left|\vec{E}_i{}^* \cdot \vec{d}\right|^2\ i = 1,2$ **(3.2)** denoting the projection of the optical field onto the direction of the dipole moment $\vec{d}$. The DOS is defined as (the absolute value of) the inverse slope of the dispersion relation [3]. As for any structure, given the transmission coefficient $t(\omega) = X(\omega) + jY(\omega) = |t(\omega)|\exp\left[j\psi(\omega)\right]$ **(3.3)**, the DOS for a CLC reads

$$\rho_i(\omega) = DOS(\omega) = \frac{1}{L}\frac{\frac{dY_i(\omega)}{d\omega}X_i(\omega) - \frac{dX_i(\omega)}{d\omega}Y_i(\omega)}{{X_i}^2(\omega) + {Y_i}^2(\omega)} \quad \textbf{(3.4)} \quad \text{for} \quad t_i(\omega) \propto \frac{(1 - m_i' - \lambda' f_i)\frac{m_i' + \lambda' f_i}{1 + m_i' + \lambda' f_i}\exp(jk_i Np)}{1 - \left(\frac{1 - m_i' - \lambda' f_i}{1 + m_i' + \lambda' f_i}\right)^2 \exp(2jk_i Np)}, i = 1,2 \quad \textbf{(3.5)}$$

In the figures that follow, we depict the DOS for the two normal light modes that propagate parallel to the helical axis as well as their relative intensity contribution. These results are obtained after performing the orientational average of the squared projections of the transition dipole moment with respect to the rotating frame planes. The degree of order is indicated by an order parameter $S_d = \langle (3/2)cos^2\theta - 1/2 \rangle$ **(3.6)**, where θ is the angle between the director and the dipole moment (for perfect alignment $S_d = 1$ while for poor alignment $S_d \to 0$).

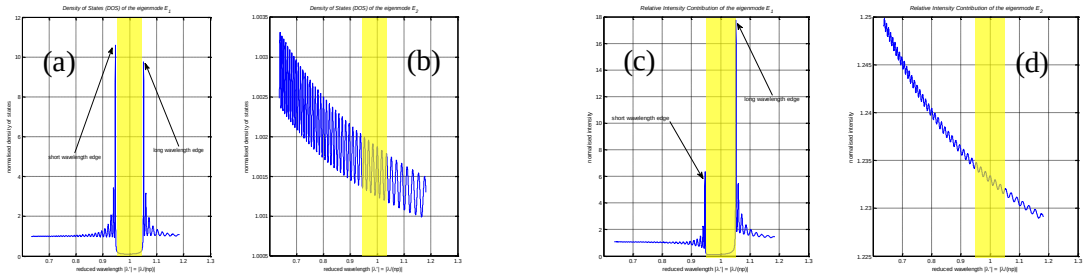

Figure 3.1: *Normalised DOS of the eigenwaves $\vec{E}_1(a)$ and $\vec{E}_2(b)$ for a CLC cell with thickness $L = 30p$ and relative dielectric anisotropy $a = 0.1$ (left). Relative intensity contributions of the eigenwaves $\vec{E}_1(c)$ and $\vec{E}_2$ (d) for a CLC cell with the same thickness and relative dielectric anisotropy and order parameter $S_d = 0.43$ (right).The yellow area marks the stop band.*

As we can observe, the DOS of the eigenwave $\vec{E}_1$ peaks at either side of the stop band (denoted as short and long-wavelength edge) and the same trend is also followed by the emission intensity (which is dependent upon the order parameter S_d). The same result can be obtained from the analysis carried out in [1], where the transmission coefficient is expressed as a ratio of the (complex) amplitude of the diffracted eigenwaves and the transmitted wave, upon the formulation of a boundary value problem. For an absorbing or an amplifying CLC structure, now, losses can be incorporated in our analysis by introducing a small (wavelength independent) imaginary part γ in the expression for the average dielectric constant $\bar{\varepsilon} = \bar{n}^2 = {\bar{n}_0}^2 + j\gamma, |\gamma| \ll 1$, **(3.7)** where a negative γ corresponds to gain and a positive γ corresponds to losses, as we have assumed an $exp(jk_i z)$ dependence for the normal modes [3]. The introduction of an imaginary part in the dielectric constant affects substantially both the reflectivity of the structure (as well as the transmittance) and the DOS.

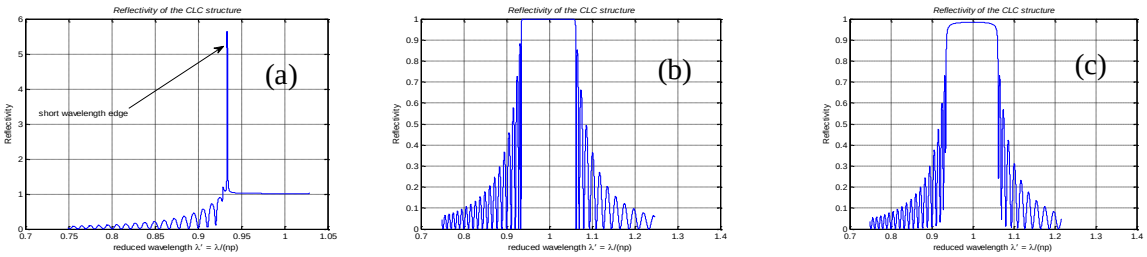

Figure 3.2:*Intensity reflection of a 30-period CLC(a) with a small negative imaginary part of the mean dielectric constant,$\gamma < 0, |\gamma| \ll 1$ $(\gamma = -0.005)$ (gain)(b)with real mean dielectric constant $(\gamma = 0)$(c) with a small positive imaginary part of the dielectric constant $\gamma > 0, |\gamma| \ll 1$ $(\gamma = 0.005)$ (losses) . In all, $a = 0.12$.*

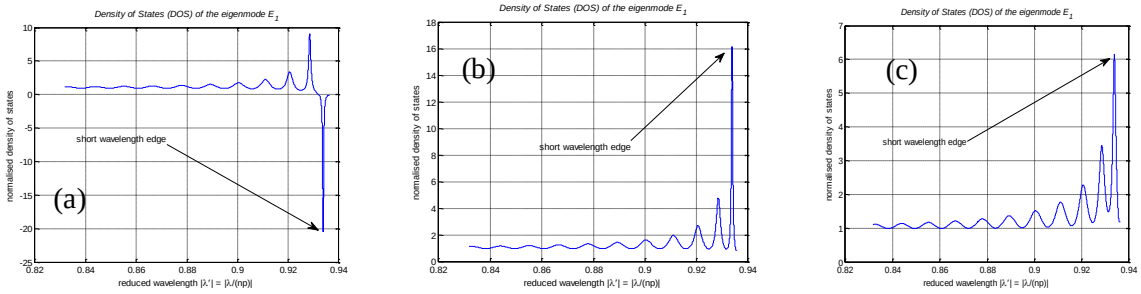

Figure 3.3: *DOS (algebraic value)of the eigenwave $\vec{E}_1$ for a 30-period CLC cell (a) with a small negative imaginary part of the mean dielectric constant $\gamma = -0.005$ (gain)(b) with real mean dielectric constant, $\gamma = 0$ (c) with a small positive imaginary part of the mean dielectric constant $\gamma = 0.005$(losses).In all cases $a = 0.12$.*

In the lossless case, the DOS increases with thickness in a parabolic fashion, which is also a well known result for wave propagation in periodic layered media[4]. The DOS decreases rapidly with losses, as also discussed in [4,5], where a relation of the form $\rho_M \sim L^2 \exp(-\beta L)$ **(3.8)** is introduced to explain the observed behaviour. The exponentially decaying term represents the incorporation of losses from the case of the Fabry-Perot resonator as an exponential multiplicative factor in the mirror reflectivities. In the figures that follow, we depict the dependence of losses on the cell thickness by introducing a small imaginary factor γ in the framework of the original analysis in [1], that modifies accordingly the real and imaginary part of the transmission coefficient.

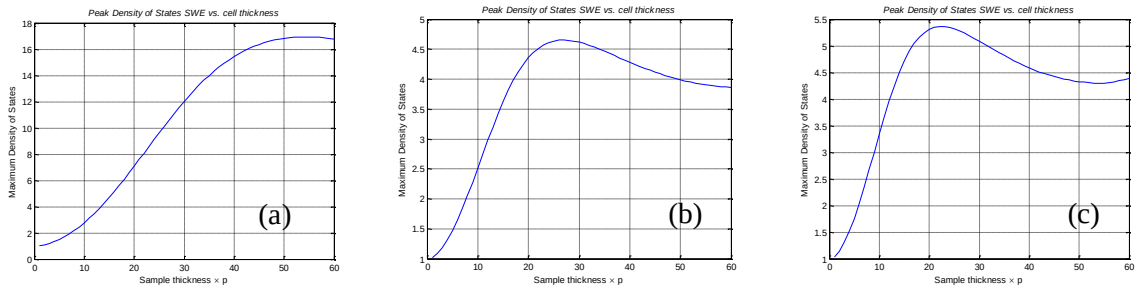

Figure 3.4: *Maximum DOS for a CLC cell (as a function of its thickness) for the eigenwave* $\vec{E}_1$ *(a) with birefringence* $\Delta n = 0.2$ *and a loss factor of* $\gamma = 0.001$ *(b) with birefringence* $\Delta n = 0.2$ *and a loss factor of* $\gamma = 0.008$ *(c) with birefringence* $\Delta n = 0.26$ *and a loss factor of* $\gamma = 0.008$.

The curves fit qualitatively the experimental data reported in [4] and [5], as to a first order approximation, the lasing threshold energy is inversely proportional to the density of states. The threshold energy, then, appears to follow the suggested form of the relation $E_{th} \sim L[A + B/(\rho L)]$ **(3.9)** in [5]. The slope efficiency is also found to have the same behaviour with the DOS. As it can be deduced, the DOS decreases dramatically with losses. When losses tend to zero, the parabolic profile is approached [4, 5]. This is similar to conventional DFB structures [4]. The DOS increases also with increased refractive index difference between alternating layers in a quarter-wave stack [6].

4. Periodic layered media: calculation of the DOS and comparison with the CLCs

Although CLCs differ substantially from a quarter dielectric stack, the DOS seems to exhibit a similar behaviour as noted in [4].We use a transfer matrix method in order to calculate the DOS, assuming that each layer of the dielectric stack is represented by a unimodular translation matrix [7].When a plane wave is incident on a periodic medium, a Bloch wave is generated [7].The analysis results in the formulation of an eigenvalue problem where the resulting eigenvalues are the expressions for the Bloch wavenumber and the eigenvectors have the complex amplitudes of the travelling plane waves as their elements. If the frequency of the impinging wave falls in the region of the stop band, then an evanescent wave is generated that cannot propagate in the medium (analogous to the case of the imaginary 'reduced index' of the first propagating eigenwave in the CLC cells). The periodic layered medium is depicted in the figure that follows

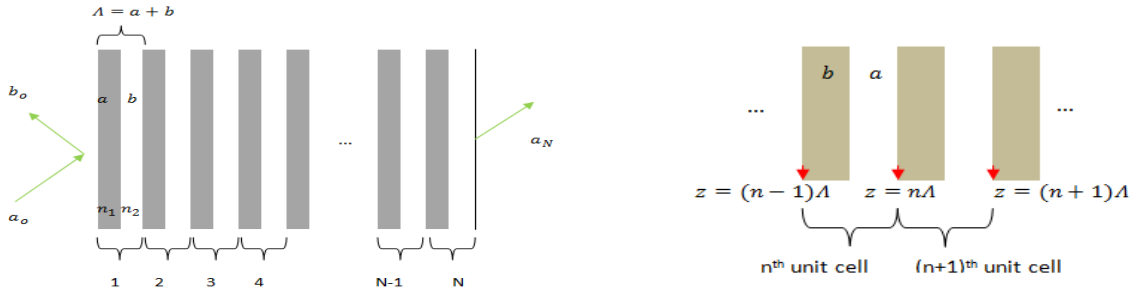

Figure 4.1: *Schematic representations of a periodic layered medium consisting of alternating layers of two different transparent materials with refractive indices* n_1 *and* n_2 *and thicknesses* a *and* b *respectively.*

For TE waves the density of states is calculated again with the aid of (3.4) for a transmission coefficient [7]

$$T_N = \left(\frac{a_N}{a_o}\right)_{b_N=0} = \frac{1}{AU_{N-1} - U_{N-2}} \quad \textbf{(4.1)} \qquad \text{with} \qquad U_N = \frac{\sin[(N+1)K\Lambda]}{\sin(K\Lambda)} \quad \textbf{(4.2)}$$

$$K(\omega, k_y) = \frac{1}{\Lambda}\cos^{-1}\left[\frac{1}{2}(A + D)\right] \quad \textbf{(4.3)} \qquad A = \exp(jk_{1z}a)\left[cos(k_{2z}b) + \frac{j}{2}\left(\frac{k_{2z}}{k_{1z}} + \frac{k_{1z}}{k_{2z}}\right) sin(k_{2z}b)\right] \quad \textbf{(4.4)}$$

$$\text{and} \quad D = \exp(-jk_{1z}a)\left[cos(k_{2z}b) - \frac{j}{2}\left(\frac{k_{2z}}{k_{1z}} + \frac{k_{1z}}{k_{2z}}\right) sin(k_{2z}b)\right] \quad \textbf{(4.5)}$$

The stop-band in these structures is the region where the Bloch wavenumber K is complex. For a quarter-wave stack, each period is an exact half-wave at the stop band centre. The z components of the wavevector read

$k_{iz} = \sqrt{\left(\frac{n_i \omega}{c}\right)^2 - k_y^2}$, $i = 1.2$ **(4.6)** where the case of oblique incidence and propagation corresponds to $k_y \neq 0$. Below, we depict the DOS and the transmission coefficient for normal and oblique incidence (and propagation) of a TE plane monochromatic wave, as a function of the angular frequency (three stop-bands are shown). In the figures that follow, ω_o denotes that centre of the photonic band-gap. We can observe a shift in the stop-bands as well as an obvious increase in the DOS for oblique propagation.

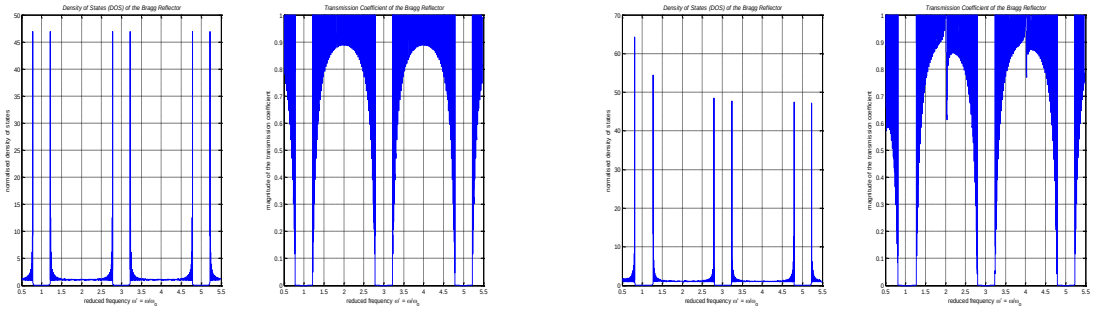

Figure 4.2: *Normalised DOS and transmission coefficient of a 30-period quarter wave Bragg reflector with* $n_1 = 1$ *and* $n_1 = 2$ *for normal incidence* ($k_y = 0$) *(left) and for oblique incidence (right). The* y *component of the wavevector of propagation (remaining constant throughout the medium) is set to* $k_y = 0.4k_o = 0.8\pi/\lambda_o$.

The results are in accordance with the graphs given in [6], where the quadratic dependence of the DOS on the cell thickness (for a non absorbing quarter-wave stack) is also reported.

Conclusions

The aim of this paper is to present important aspects of laser emission in CLC structures, emphasising the significance of the DOS in identifying the key parameters that must be addressed in designing low threshold, high efficiency lasers. One must consider variations in the DOS and transmission characteristics of such structures with a multitude of parameters and situations (e.g. cell thickness, oblique propagation, different gain profiles of the fluorescent dye molecules amongst others) bearing in mind that CLCs are an absorbing medium for the pumping wave but an amplifying one for the emitted wave. Other DFB structures have proved to be good guides for predicting the behaviour of the DOS in CLCs despite their differences. In particular, the effect of anomalous absorption under the presence of gain is also reported in [1] as well as in the case of conventional DFB structures [7]. Furthermore, determining the DOS will be an essential tool for studying propagation characteristics of oblique modes in CLC structures.

References

[1] V. A. Belyakov and S. V. Semenov, 'Optical Edge Modes in Photonic Liquid Crystals', JETP, Vol. 109, No. 4, 687-699 (2009)

[2] Hl. de Vries, 'Rotatory Power and Other Optical Properties of Certain Liquid Crystals', Acta Cryst. 4, 219-226 (1951)

[3] J. Schmidtke and W. Stille, 'Fluorescence of a dye-doped cholesteric liquid crystal film in the region of the stop band: theory and experiment', Eur. Phys J. B 31, 179-194 (2003)

[4] M. F. Moreira, S. Relaix, W. Cao, B. Taheri and B. Palffy-Muhoray, 'Mirrorless lasing and lasing thresholds in cholesteric liquid crystals', Liquid Crystal Microlasers, Chapter 12, 223-240, Transworld Research Network, 2010

[5] S. M. Morris, A.D. Ford, G. Gillepsie, M. N. Pivnenko, O. Hadeler and H. J. Coles, 'The Emission Characteristics of Liquid Crystal Lasers', J. SID, 14(6),565-573 (2006)

[6] J. M. Bendickson, J. P. Dowling and M. Scalora, 'Analytic expressions for the electromagnetic mode density in finite, one-dimensional, photonic band-gap structures', Phys. Rev. E53, 4107 (1996)

[7] A. Yariv and P. Yeh, 'Photonics: Optical Electronics in Modern Communications', 6th edition, Oxford University Press, 2007, ISBN 0-19-517946-3